HENRY
Hydraulic Engineering Repository

Ein Service der Bundesanstalt für Wasserbau

Conference Paper, Published Version

Jae Oh, Seung; Briaud, Jean-Louis; Chang, Kuang-An; Chen, Hamn-Ching

Maximum Abutment Scour Depth in Cohesive Soils

Verfügbar unter/Available at: https://hdl.handle.net/20.500.11970/100243

Vorgeschlagene Zitierweise/Suggested citation:
Jae Oh, Seung; Briaud, Jean-Louis; Chang, Kuang-An; Chen, Hamn-Ching (2010): Maximum Abutment Scour Depth in Cohesive Soils. In: Burns, Susan E.; Bhatia, Shobha K.; Avila, Catherine M. C.; Hunt, Beatrice E. (Hg.): Proceedings 5th International Conference on Scour and Erosion (ICSE-5), November 7-10, 2010, San Francisco, USA. Reston, Va.: American Society of Civil Engineers. S. 132-141.

Standardnutzungsbedingungen/Terms of Use:

Die Dokumente in HENRY stehen unter der Creative Commons Lizenz CC BY 4.0, sofern keine abweichenden Nutzungsbedingungen getroffen wurden. Damit ist sowohl die kommerzielle Nutzung als auch das Teilen, die Weiterbearbeitung und Speicherung erlaubt. Das Verwenden und das Bearbeiten stehen unter der Bedingung der Namensnennung. Im Einzelfall kann eine restriktivere Lizenz gelten; dann gelten abweichend von den obigen Nutzungsbedingungen die in der dort genannten Lizenz gewährten Nutzungsrechte.

Documents in HENRY are made available under the Creative Commons License CC BY 4.0, if no other license is applicable. Under CC BY 4.0 commercial use and sharing, remixing, transforming, and building upon the material of the work is permitted. In some cases a different, more restrictive license may apply; if applicable the terms of the restrictive license will be binding.

Maximum Abutment Scour Depth in Cohesive Soils

Seung Jae Oh[1], Jean-Louis Briaud[2], Kuang-An Chang[3], Hamn-Ching Chen[4]

[1] Ph.D., Research Assistant, Texas A&M University, Department of Civil Engineering, College Station, TX 77843-3136, seungjaeo@gmail.com
[2] Professor, Texas A&M University, Department of Civil Engineering, College Station, TX 77843-3136, briaud@tamu.edu
[3] Associate Professor, Texas A&M University, Department of Civil Engineering, College Station, TX 77843-3136, kchang@civil.tamu.edu
[4] Professor, Texas A&M University, Department of Civil Engineering, College Station, TX 77843-3136, hcchen@civil.tamu.edu

ABSTRACT: Most conventional methods to predict the depth of abutment scour were developed with flume test results using cohesionless soils, and those methods have been used to the abutment scour depth prediction in cohesive soils. Generally floodplains where most abutments are located are composed of less erodible soils such as cohesive soils. Therefore those methods usually predict overly conservative scour depths. For the cost effective designs, a series of flume tests were carried out using Porcelain clay. Based on dimensional analysis and the test results, a new method to predict the bridge abutment scour depths is proposed. The new method built on the difference between the local Froude number and the critical Froude number. Because abutment scour occurs only when the local velocity is higher than the critical velocity which is the maximum velocity the channel bed material can withstand.

INTRODUCTION

Floodplains where most bridge abutments exist are typically composed of cohesive soils such as silts and clays. The soil properties of cohesive soils on erosion resistance are much complicated than those of cohesionless soils. Cohesionless soils resist erosion by buoyant weight and the soil particle friction, while cohesive soils do it by electromagnetic and electrostatic interparticle forces (Briaud et al. 1999b). The critical shear stress, which is the maximum shear stress soil particles can resist from the flow, of uniformly distributed cohesionless soils linearly decreases with particle size decrease. On the contrary, the critical shear stress of cohesive soils cannot be defined by the particle size (Briaud et al. 2001). Moreover, the erosion rate of cohesive soils can be 1,000 times slower than that of coehsionless soils, and a few days may generate only a small fraction of the maximum scour depth (Briaud et al. 2004). Hence, both the critical velocity and the scour rate should be considered in the prediction of scour depth in cohesive material for more accurate and economic bridge design and maintenance, and these requirements stimulated to the development of the SRICOS-EFA (Scour Rate In Cohesive Soils – Erosion Function Apparatus) method.

The SRICOS-EFA method was initially developed to predict the depth around single circular pier in cohesive soil (Briaud et al. 1999b). It was further developed to predict complex pier scour and contraction scour (Briaud et al. 2004). Moreover,

more complicated but realistic geological and hydrological conditions were considered (Briaud et al. 1999a).

In the present study a method to predict the maximum abutment scour depth in cohesive soils is introduced to extend the use of the SRICOS-EFA method to the scour depth prediction around the toe of abutment. The method was developed using the results of a series of large flume tests for abutment scour in cohesive soils.

PREVIOUS STUDIES ON MAXIMUM ABUTMENT SCOUR DEPTH

Since most prediction methods to predict abutment scour depths are developed flume test results using cohesionless soils, many equations include soil particle sizes to define the critical shear stress or erodibility.

Froehlich's study

Froehlich (1989) collected abutment scour test results taken by other researchers in rectangular channels in different laboratories from 1953 to 1985, and performed data regression using a total of 164 clear-water and 170 live-bed abutment scour measurements in sand. He proposed both the live-bed and the clear-water abutment scour equation as follows:

Clear-water scour:

$$\frac{y_{s(Abut)}}{y_1} = 0.78 \cdot K_1 \cdot K_2 \cdot \left(\frac{L'}{y_1}\right)^{0.63} \left(\frac{y_1}{D_{50}}\right)^{0.43} Fr_1^{1.16} \sigma_g^{-1.87} \quad (1)$$

Live-bed scour:

$$\frac{y_{s(Abut)}}{y_1} = 2.27 \cdot K_1 \cdot K_2 \cdot \left(\frac{L'}{y_1}\right)^{0.43} Fr_1^{0.61} \quad (2)$$

where $\sigma_g = \left(D_{84}/D_{16}\right)^{0.5}$ is the geometric standard deviation of the bed material, and D_{16}, D_{50}, and D_{84} are the particle size for 16, 50 and 84 percentile of weight, respectively, $Fr_1 = \left(V_1 / \sqrt{g \cdot y_1}\right)$ is Froude number based on approach water depth and approach velocity, K_1 is the correction factor for abutment shape that has a value of 1.0, 0.82 and 0.55 for vertical wall, wing-wall, and spill-through abutment, respectively. K_2 is the correction factor for the alignment of the abutment with respect to the flow direction ($K_2 = \left(\theta/90\right)^{0.13}$) with θ being the angle of abutment alignment (the embankment is skewed downstream if $\theta < 90°$, and skewed upstream if $\theta > 90°$, L' is the average length of abutment ($L' = A_e / y_1$ with A_e being the flow area obstructed by the embankment), y_1 is the water depth in the approach section, and $y_{s(Abut)}$ is the maximum abutment scour depth

Sturm's study

Sturm (2004) conducted a series of flume tests and analyzed test results of bridge abutment scour depths in compound channels. The equation of the maximum abutment scour depth in the compound channel was suggested as:

$$\frac{y_{s(Abut)}}{y_{f0}} = 8.14\left[\frac{q_{f1}}{M \cdot q_{fc0}} - 0.4\right] \tag{3}$$

where M is the discharge contraction ratio defined as $M = (Q - Q_{block})/Q$ with Q being the total discharge and Q_{block} being the discharge blocked by the approach embankment, $q_{f1}(=V_{f1} \cdot y_{f1})$ is the unit flow rate at the approach section with the effect of backwater induced by the abutment, $q_{fc0}(=V_{fc0} \cdot y_{f0})$ is the critical unit flow rate on the floodplain without the effect of backwater, V_{f1} is the approach average velocity on the floodplain, $V_{fc0}\left(= 1/k_n \cdot \sqrt{(Gs-1)\tau_{*c}} D_{50}^{1/3} y_{f0}^{1/6}\right)$ is the critical velocity on the floodplain without backwater effect, Gs is the specific gravity of cohesionless soil, k_n is constant in Strickler-type relationship for Manning's n $\left(n = k_n D_{50}^{1/6}\right)$, τ_{*c} is the critical value of Shields' parameter, y_{f0} is water depth on floodplain without backwater effect, and y_{f1} is the approach water depth on the floodplain.

SRICOS-EFA METHOD

The principle of the SRICOS-EFA method is summarized here to provide a necessary background. The SRICOS-EFA method is highly dependent on the maximum scour depth and the shear stress between the flow and soil interface. The methodology of maximum scour depth is developed by flume test results, and the maximum shear stress on the channel bed is developed by three-dimensional numerical simulations. The procedure of SRICOS method is consisted with following steps.

(1) Obtain standard 76.2 mm diameter Shelby tube samples as close to the bridge support as possible.
(2) Conduct EFA test (Briaud et al. 1999a) of the samples to obtain the critical shear stress (τ_c) and the erodibility curve of erosion rate versus shear stress ($\dot{z}$ vs. τ).
(3) Determine the maximum shear stress τ_{max}.
(4) Obtain the initial scour rate $(\dot{z}_i)$ corresponding to τ_{max}.
(5) Develop the complete scour depth y_s vs. t curve.
(6) Predict the depth of scour by reading the y_s vs. t at the time corresponding to the duration of the flood using

$$y_s(t) = \frac{t}{\frac{1}{\dot{z}_i} + \frac{t}{y_s}} \tag{4}$$

where t is time (hour), and y_s is the maximum scour depth.

EXPERIMENTS

A concrete flume with dimension of 45.7 m in length, 3.7 m in width and 3.4 m in depth was used to conduct the abutment scour tests. A sediment pit, which has dimensions of 7.5 m in length, 3.7 m in width and 1.5 m in depth, is located around the middle of the flume. The pit was filled with the Porcelain clay, and the geotechnical properties of the clay are given in Table 1. The Porcelain clay is classified as CL (clay with low plasticity) by ASTM D-2487. The critical shear stress of the Porcelain clay was obtained after 11 EFA (Erosion Function Apparatus) tests as $\tau_c = 0.8$ Pa.

Table 1 – Geotechnical properties of the Porcelain clay.

Property	Average	Property	Average
Liquid Limit	30.7 %	Initial water content	25 %
Plastic Limit	16.6 %	Median grain size (D_{50})	0.0035 mm
Plasticity Index	14.1 %	Undrained shear stress	21.2 kPa

Two types of channel were used for flume tests: one is a rectangular channel, and the other is a compound channel. The channel cross sections are shown in Figure 1. Three types of abutment made of plywood were used in the flume tests: the first one is the wing wall shape, the second one is the spill-through shape with a 2(H):1(V) slope, and the third one is the spill-through shape with a 3(H):1(V) slope.

A point gauge was used to measure the water depth and the maximum scour depth, and a bed profiler was used to scan the channel bottom topography. The velocity was measured at the 60% of water depth from the free surface by two side looking 3-D ADVs (Acoustic Doppler Velocimeters).

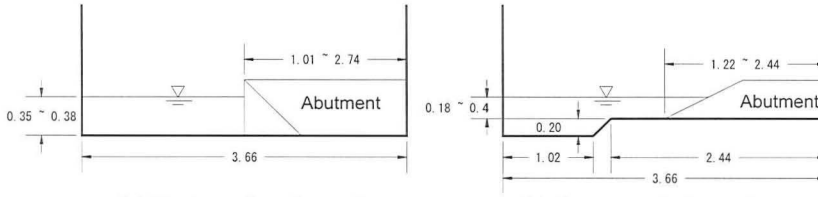

(a) Rectangular channel **(b) Compound channel**

Figure 1 – Cross sectional views of channel configuration. (units: meter)

TEST RESULTS

Eighteen flume tests were conducted by varying the abutment shape, approach embankment length, abutment alignment, channel shape, water depth and flow velocity. During each test the channel bottom was scanned as many times as possible, and the maximum scour depth in each measurement ($y_{s(Abut)}(t)$) was recorded because scour develops very slowly in cohesive soil. This is different with scour development in cohesionless soil. Velocity was measured at the beginning, approximately 100 hours after the test started, and before end of the test.

Figure 2(a) shows the pattern of time average velocity, and Figure 2(b) shows the pattern of the turbulence intensity ($TI = \sqrt{\sigma_x^2 + \sigma_y^2 + \sigma_z^2}$ where σ is the standard deviation of measured velocity and the subscription x, y and z are the direction of flow) at the beginning of the test. The change of channel bottom bathymetry during the test is given in Figure 3. The maximum average velocity was found to be close to the wall which is away from and downstream of the abutment (dashed circle in Figure 2(a)), while the highest turbulence intensity was around the toe of the abutment at slightly downstream (dashed circle in Figure 2(b)). These patterns are coincident with locations at which the deepest contraction scour and the abutment scour were measured during every measurement (Figure 3).

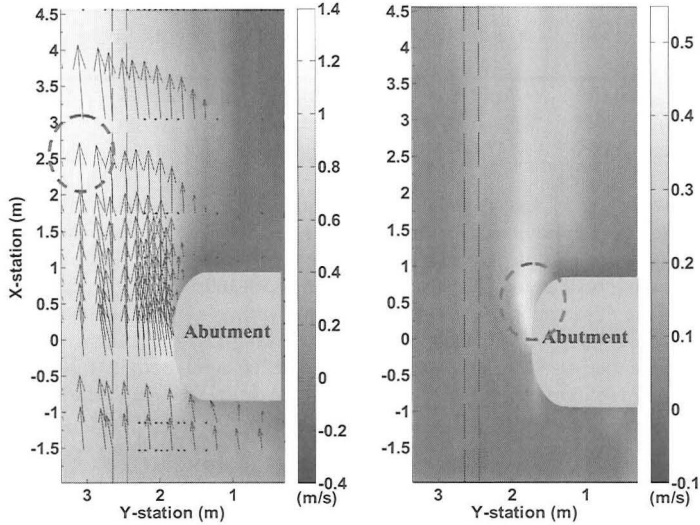

(a) Time averaged velocity (b) Turbulence intensity

Figure 2 – Pattern of velocity in the beginning of test.

The scour depth was recorded as a function of time as $y_{s(Abut)}(t)$. At the end of each test, the scour depth was still developing although the test time is longer than 300 hours (Figure 3 and Figure 4). It is therefore not feasible to obtain the maximum scour depth directly through the test. A hyperbolic model was thus used to obtain the maximum abutment scour depths (Figure 4).

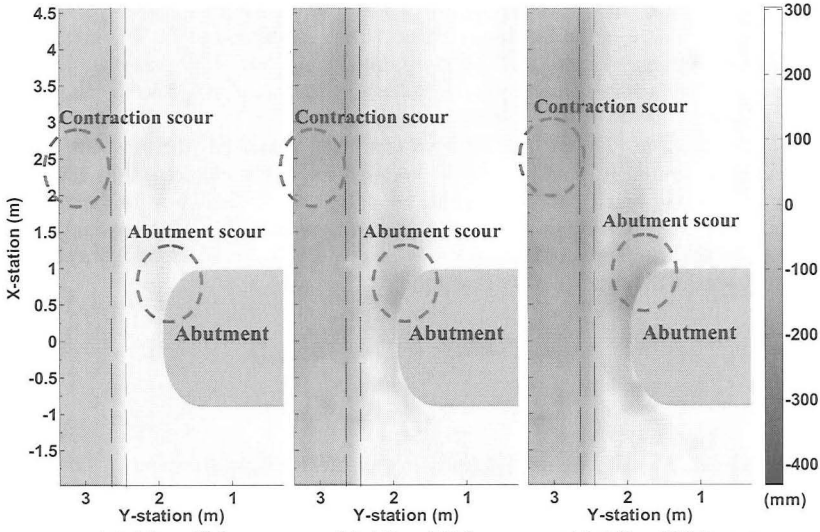

(a) After 60 hours (b) After 189 hours (c) After 320 hours

Figure 3 – Scour development.

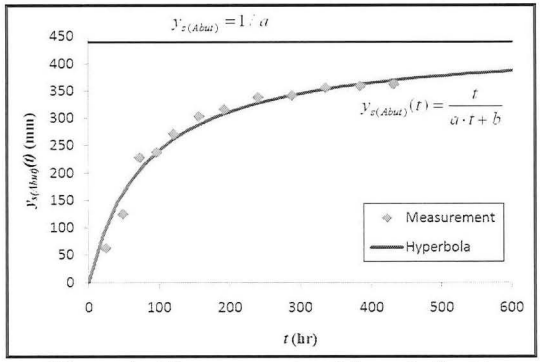

Figure 4 – Measurement and hyperbolic fit.

During experiments, it was found that the maximum scour depth, in the same test conditions except abutment shape, of the 2(H):1(V) spill through abutment is 70% of that of the wing-wall abutment. This ratio is close to the abutment shape correction factor between the spill-through abutment and the wing-wall abutment in Melville (1992). However, contrary results were found in the abutment alignment effect to previous studies (Froehlich 1989; Melville 1992; Richardson and Davis 1995). The maximum scour depth for the abutment skewed upstream is less than that for the abutment normally aligned to the flow. The contrary may be due to the use of different types of abutment. The spill-through abutment which induces a relatively

smooth flow around the toe of the abutment was used in this study, whereas vertical abutments were used in the previous studies. This is evidenced in *TI*. The maximum *TI* for the abutment with $\theta = 120°$ was approximately 10% less than that for the abutment with $\theta = 90°$. Note that the turbulence pattern is identical to the abutment scour pattern.

As shown in Figure 2 and Figure 3, the local velocity is the most important parameter on abutment scour. However, it cannot be easily calculated. In addition, flume tests cannot account for all possible conditions in the field. For the calculation of the local velocity around the abutment, the approximation in Maryland SHA Bridge Scour Program (*ABSCOUR*) was adopted. The method to convert the hydraulic data to the local velocity is as follows:

$$V_{f2} = \begin{cases} Q/A_2, \text{ for short setback } \left((L_f - L') \le 5y_{m1}\right) \\ Q_{fp1}/A_{f2}, \text{ for long setback } \left(L' \le 0.25L_f\right) \\ \text{otherwise use a linearly interpolated velocity between} \\ Q/A_2 \text{ for } (L_f - L') = 5y_{m1} \text{ and } Q_{fp1}/A_{f2} \text{ for } L' = 0.25L_f \end{cases} \quad (5)$$

where Q_{fp1} is the discharge on the floodplain at the approach section immediately upstream of the abutment, A_2 is total flow area at the contracted section, A_{f2} is the flow area on the floodplain at the contracted section, and L_f is the width of floodplain at the approach section, and y_{m1} is the water depth of main channel at the approach section.

DIMENSIONAL ANALYSIS

The variables affecting abutment scour can be expressed in equation (6) and rewritten in dimensionless form in equation (7) below.

$$y_{s(Abut)} = f(y_{m1}, y_{f1}, L_f, L', Sh, \theta, g, V_{f2}, \mu, V_{fc}) \quad (6)$$

$$\frac{y_{s(Abut)}}{y_{f1}} = f\left(\frac{L_f - L'}{y_{f1}}, Sh, \theta, Fr_{f2}, Fr_{fc}, \mathrm{Re}_{f2}\right) \quad (7)$$

where Sh is the abutment shape, θ is the alignment angle of abutment, μ is the viscosity of water, $Fr_{f2} = \frac{V_{f2}}{\sqrt{gy_{f1}}}$, $Fr_{fc} = \frac{V_{fc}}{\sqrt{gy_{f1}}}\frac{\sqrt{\tau_c/\rho}}{gny_{f1}^{1/3}}$, and $\mathrm{Re}_{f2} = \frac{\rho y_f V_{f2}}{\mu}$

Abutment scour occurs when the local flow velocity is higher than the critical velocity, and continues until the local velocity equals to the critical velocity. Thus the

abutment scour equation may be expressed in the form of Froude number difference as follows:

$$\frac{y_{s(Abut)}}{y_{f1}} = K_1 \cdot K_2 \cdot K_L \cdot K_G \cdot K_{\mathrm{Re}} \cdot \alpha_1 \cdot \left(\beta_1 \cdot Fr_{f2} - Fr_{fc}\right)^{\chi_1} \tag{8}$$

where K_L is the correction factor for the abutment location, K_G is the correction factor for the channel geometry, K_{Re} is the correction factor for the Reynolds number effect, and α_1 , β_1 and χ_1 are constant.

In equation (8), the three constants (α_1, β_1 and χ_1) and four correction factors (K_1, K_2, K_L and K_G) were obtained after data regression using flume test results. They are as follows:

$$\frac{y_{s(Abut)}}{y_{f1}} = K_1 \cdot K_2 \cdot K_L \cdot K_G \cdot 7.94 \cdot \left(1.65 \cdot Fr_{f2} - Fr_{fc}\right) \tag{9}$$

$$K_1 = \begin{cases} 1.22 & \text{for vertical-wall abutment} \\ 1.0 & \text{for wing-wall abutment} \\ 0.73 & \text{for spill-through abutment with 2:1 Slope} \\ 0.59 & \text{for spill-through abutment with 3:1 Slope} \end{cases}$$

$$K_2 = \begin{cases} 1.0 - 0.005\left|\theta - 90°\right| & \text{for } 60° \le \theta \le 120° \\ 0.85 & \text{otherwise} \end{cases}$$

$$K_G = \begin{cases} 1.0 & \text{for compound channel} \\ 0.42 & \text{for rectangular channel} \end{cases}$$

$$K_L = \begin{cases} -0.23\dfrac{L_f - L'}{y_{f1}} + 1.35 & \text{for } \dfrac{L_f - L'}{y_{f1}} < 1.5 \\ 1.0 & \text{otherwise} \end{cases}$$

In equation (9), the correction factors for the Reynolds number effect was not obtained using the 18 flume test results because the range of Reynolds numbers in the tests are too narrow. As expected, equation (9) fits well to the flume test results of the present study while mostly under estimates when compared with smaller scale laboratory test and over estimates when compared with field data. The main cause of the discrepancy is the Reynolds number effect. The range of Reynolds number in several studies, including the present study, is given in Table 2.

Table 2 – Range of Reynolds numbers (Re_{f2}) in studies

	Froehlich (1989)	Sturm (2004)	Present study	Benedict et al. (2006)
Min. Re_{f2}	7,425	8,433	102,511	143,500
Max. Re_{f2}	71,133	55,451	322,681	11,436,281
Avg. Re_{f2}	50,073	28,248	219,837	2,782,622

Figure 5 shows the effect of Reynolds number on the maximum abutment scour depth. In order to quantify the effect, laboratory data in Table 2 from Froehlich (1989) and Strum (2004) were plotted. Note that the database from Benedict et al. (2006) was not used because the accuracy of the field data is likely to be much lower than that of the laboratory test. According to the curve fitting shown in Figure 5, the effect of Reynolds number can be expressed as

$$K_{\mathrm{Re}} = \frac{1}{0.033 \cdot \mathrm{Re}_{f2}^{0.28}} \tag{10}$$

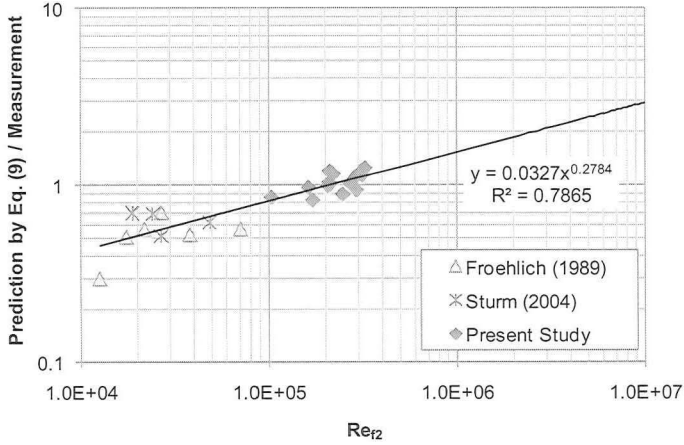

Figure 5 – The effect of Reynolds number in maximum abutment scour depth.

Accordingly, the equation for the maximum abutment scour prediction becomes:

$$\begin{aligned} \frac{y_{s(Abut)}}{y_{f1}} &= K_1 \cdot K_2 \cdot K_L \cdot K_G \cdot K_{\mathrm{Re}} \cdot 7.94 \cdot \left(1.65 \cdot Fr_{f2} - Fr_{fc}\right) \\ &= K_1 \cdot K_2 \cdot K_L \cdot K_G \cdot 243 \cdot \mathrm{Re}_{f2}^{-0.28} \cdot \left(1.65 \cdot Fr_{f2} - Fr_{fc}\right) \end{aligned} \tag{8}$$

CONCLUSION

A series of flume test were conducted for the abutment scour in cohesive soils. A method to predict the maximum abutment scour depth is proposed using the flume test results. The method is based on the difference between the local Froude number and the critical Froude number. Four correction factors, abutment shape, alignment, channel geometry, and abutment location, were included. The scale effect is also considered.

ACKNOWLEDGEMENT

This work was supported by NCHRP (Project No. 24-15(2)). Mr. Stanley R. Davis and Mr. David Reynaud are the technical contacts. Their help are specially thanked.

REFERENCES

ABSCOUR. (Maryland SHA Bridge Scour Computer Program), Maryland State Highway Administration, Version 8, build 1.02, compiled August 14, 2006.

ASTM D2487, American Society for Testing and Materials, Philadelphia, USA

Benedict, S. T., Deshpande, N., Aziz, N.M., and Conrads, P.A. (2006). "Trends of Abutment-Scour Prediction Equation Applied to 144 Field Sites in Scour Carolina." *Open-File Report 03-295*, U.S. Geological Survey, http://pubs.water.usgs.gov/ofr2003-295/ [retrieved 10 January 2009]

Briaud, J.-L., Chen, H. C., Li, Y., Nurtjahyo, P., and Wang, J. (2004). "Pier and Contraction Scour in Cohesive Soils." *NCHRP Report 516*, Transportation Research Board, Washington, D.C.

Briaud, J.-L., Ting, F., Chen, H. C., Cao, Y., Han, S.-W., and Kwak, K. (2001). "Erosion Function Apparatus for Scour Rate Predictions." *J. Geotech. Geoenviron. Eng.*, 127(2), 105-113.

Briaud, J.-L., Ting, F., Chen, H. C., Gudavalli, S. R., Kwak, K., Philogene, B., Han, S.-W., Perugu, S., Wei, G., Nurtjahyo, P., Cao, Y., and Li, Y. (1999a). "SRICOS: Prediction of scour rate at bridge piers." *TTI Report No. 2937-1 to the Texas DOT*, Texas A&M University, College Station, TX, USA.

Briaud, J.-L., Ting, F., Chen, H. C., Gudavalli, S. R., Perugu, S., and Wei, G. (1999b). "SRICOS: Prediction of scour rate in cohesive soils at bridge piers." *J. Geotech. Geoenviron. Eng.*, 125(4), 237-246.

Froehlich, D. C. "Local Scour at Bridge Abutment." *Proceedings of National Conference on Hydraulic Engineering*, 1989, New York, NJ, USA, 13-18.

Melville, B. W. (1992). "Local Scour at Bridge Abutment." *J. Hydraulic Eng.*, 118(4), 615-631.

Richardson, E. V., and Davis, S. M. (1995). "Evaluating Scour at Bridges." *FHWA-IP-90-017, HEC No. 18*, US Department of Transportation, Washington, D.C.

Strum, T. W. (2004). "Enhanced Abutment Scour Studies for Compound Channels." *FHWA-RD-99-156*, Georgia Institute of Technology, School of Civil and Environmental Engineering, Atlanta, GA 30332.